

Observation of the Semileptonic Decays $B \rightarrow D^* \tau^- \bar{\nu}_\tau$ and Evidence for $B \rightarrow D \tau^- \bar{\nu}_\tau$

B. Aubert,¹ M. Bona,¹ D. Boutigny,¹ Y. Karyotakis,¹ J. P. Lees,¹ V. Poireau,¹ X. Prudent,¹ V. Tisserand,¹ A. Zghiche,¹ J. Garra Tico,² E. Grauges,² L. Lopez,³ A. Palano,³ M. Pappagallo,³ G. Eigen,⁴ B. Stugu,⁴ L. Sun,⁴ G. S. Abrams,⁵ M. Battaglia,⁵ D. N. Brown,⁵ J. Button-Shafer,⁵ R. N. Cahn,⁵ Y. Groysman,⁵ R. G. Jacobsen,⁵ J. A. Kadyk,⁵ L. T. Kerth,⁵ Yu. G. Kolomensky,⁵ G. Kukartsev,⁵ D. Lopes Pegna,⁵ G. Lynch,⁵ L. M. Mir,⁵ T. J. Orimoto,⁵ I. L. Osipenko,⁵ M. T. Ronan,^{5,*} K. Tackmann,⁵ T. Tanabe,⁵ W. A. Wenzel,⁵ P. del Amo Sanchez,⁶ C. M. Hawkes,⁶ A. T. Watson,⁶ H. Koch,⁷ T. Schroeder,⁷ D. Walker,⁸ D. J. Asgeirsson,⁹ T. Cuhadar-Donszelmann,⁹ B. G. Fulsom,⁹ C. Hearty,⁹ T. S. Mattison,⁹ J. A. McKenna,⁹ M. Barrett,¹⁰ A. Khan,¹⁰ M. Saleem,¹⁰ L. Teodorescu,¹⁰ V. E. Blinov,¹¹ A. D. Bukin,¹¹ V. P. Druzhinin,¹¹ V. B. Golubev,¹¹ A. P. Onuchin,¹¹ S. I. Serednyakov,¹¹ Yu. I. Skovpen,¹¹ E. P. Solodov,¹¹ K. Yu. Todyshev,¹¹ M. Bondioli,¹² S. Curry,¹² I. Eschrich,¹² D. Kirkby,¹² A. J. Lankford,¹² P. Lund,¹² M. Mandelkern,¹² E. C. Martin,¹² D. P. Stoker,¹² S. Abachi,¹³ C. Buchanan,¹³ J. W. Gary,¹⁴ F. Liu,¹⁴ O. Long,¹⁴ B. C. Shen,^{14,*} G. M. Vitug,¹⁴ L. Zhang,¹⁴ H. P. Paar,¹⁵ S. Rahatlou,¹⁵ V. Sharma,¹⁵ J. W. Berryhill,¹⁶ C. Campagnari,¹⁶ A. Cunha,¹⁶ B. Dahmes,¹⁶ T. M. Hong,¹⁶ D. Kovalskyi,¹⁶ J. D. Richman,¹⁶ T. W. Beck,¹⁷ A. M. Eisner,¹⁷ C. J. Flacco,¹⁷ C. A. Heusch,¹⁷ J. Kroseberg,¹⁷ W. S. Lockman,¹⁷ T. Schalk,¹⁷ B. A. Schumm,¹⁷ A. Seiden,¹⁷ M. G. Wilson,¹⁷ L. O. Winstrom,¹⁷ E. Chen,¹⁸ C. H. Cheng,¹⁸ F. Fang,¹⁸ D. G. Hitlin,¹⁸ I. Narsky,¹⁸ T. Piatenko,¹⁸ F. C. Porter,¹⁸ R. Andreassen,¹⁹ G. Mancinelli,¹⁹ B. T. Meadows,¹⁹ K. Mishra,¹⁹ M. D. Sokoloff,¹⁹ F. Blanc,²⁰ P. C. Bloom,²⁰ S. Chen,²⁰ W. T. Ford,²⁰ J. F. Hirschauer,²⁰ A. Kreisel,²⁰ M. Nagel,²⁰ U. Nauenberg,²⁰ A. Olivas,²⁰ J. G. Smith,²⁰ K. A. Ulmer,²⁰ S. R. Wagner,²⁰ J. Zhang,²⁰ A. M. Gabareen,²¹ A. Soffer,^{21,†} W. H. Toki,²¹ R. J. Wilson,²¹ F. Winklmeier,²¹ D. D. Altenburg,²² E. Feltresi,²² A. Hauke,²² H. Jasper,²² J. Merkel,²² A. Petzold,²² B. Spaan,²² K. Wacker,²² V. Klose,²³ M. J. Kobel,²³ H. M. Lacker,²³ W. F. Mader,²³ R. Nogowski,²³ J. Schubert,²³ K. R. Schubert,²³ R. Schwierz,²³ J. E. Sundermann,²³ A. Volk,²³ D. Bernard,²⁴ G. R. Bonneaud,²⁴ E. Latour,²⁴ V. Lombardo,²⁴ Ch. Thiebaux,²⁴ M. Verderi,²⁴ P. J. Clark,²⁵ W. Gradl,²⁵ F. Muheim,²⁵ S. Playfer,²⁵ A. I. Robertson,²⁵ J. E. Watson,²⁵ Y. Xie,²⁵ M. Andreotti,²⁶ D. Bettoni,²⁶ C. Bozzi,²⁶ R. Calabrese,²⁶ A. Cecchi,²⁶ G. Cibinetto,²⁶ P. Franchini,²⁶ E. Luppi,²⁶ M. Negrini,²⁶ A. Petrella,²⁶ L. Piemontese,²⁶ E. Prencipe,²⁶ V. Santoro,²⁶ F. Anulli,²⁷ R. Baldini-Ferrolì,²⁷ A. Calcaterra,²⁷ R. de Sangro,²⁷ G. Finocchiaro,²⁷ S. Pacetti,²⁷ P. Patteri,²⁷ I. M. Peruzzi,^{27,‡} M. Piccolo,²⁷ M. Rama,²⁷ A. Zallo,²⁷ A. Buzzo,²⁸ R. Contri,²⁸ M. Lo Vetere,²⁸ M. M. Macri,²⁸ M. R. Monge,²⁸ S. Passaggio,²⁸ C. Patrignani,²⁸ E. Robutti,²⁸ A. Santroni,²⁸ S. Tosi,²⁸ K. S. Chaisanguanthum,²⁹ M. Morii,²⁹ J. Wu,²⁹ R. S. Dubitzky,³⁰ J. Marks,³⁰ S. Schenk,³⁰ U. Uwer,³⁰ D. J. Bard,³¹ P. D. Dauncey,³¹ R. L. Flack,³¹ J. A. Nash,³¹ W. Panduro Vazquez,³¹ M. Tibbetts,³¹ P. K. Behera,³² X. Chai,³² M. J. Charles,³² U. Mallik,³² J. Cochran,³³ H. B. Crawley,³³ L. Dong,³³ V. Eyges,³³ W. T. Meyer,³³ S. Prell,³³ E. I. Rosenberg,³³ A. E. Rubin,³³ Y. Y. Gao,³⁴ A. V. Gritsan,³⁴ Z. J. Guo,³⁴ C. K. Lae,³⁴ A. G. Denig,³⁵ M. Fritsch,³⁵ G. Schott,³⁵ N. Arnaud,³⁶ J. Béguilleux,³⁶ A. D'Orazio,³⁶ M. Davier,³⁶ G. Grosdidier,³⁶ A. Höcker,³⁶ V. Lepeltier,³⁶ F. Le Diberder,³⁶ A. M. Lutz,³⁶ S. Pruvot,³⁶ S. Rodier,³⁶ P. Roudeau,³⁶ M. H. Schune,³⁶ J. Serrano,³⁶ V. Sordini,³⁶ A. Stocchi,³⁶ L. Wang,³⁶ W. F. Wang,³⁶ G. Wormser,³⁶ D. J. Lange,³⁷ D. M. Wright,³⁷ I. Bingham,³⁸ J. P. Burke,³⁸ C. A. Chavez,³⁸ J. R. Fry,³⁸ E. Gabathuler,³⁸ R. Gamet,³⁸ D. E. Hutchcroft,³⁸ D. J. Payne,³⁸ K. C. Schofield,³⁸ C. Touramanis,³⁸ A. J. Bevan,³⁹ K. A. George,³⁹ F. Di Lodovico,³⁹ R. Sacco,³⁹ G. Cowan,⁴⁰ H. U. Flaecher,⁴⁰ D. A. Hopkins,⁴⁰ S. Paramesvaran,⁴⁰ F. Salvatore,⁴⁰ A. C. Wren,⁴⁰ D. N. Brown,⁴¹ C. L. Davis,⁴¹ J. Allison,⁴² N. R. Barlow,⁴² R. J. Barlow,⁴² Y. M. Chia,⁴² C. L. Edgar,⁴² G. D. Lafferty,⁴² T. J. West,⁴² J. I. Yi,⁴² J. Anderson,⁴³ C. Chen,⁴³ A. Jawahery,⁴³ D. A. Roberts,⁴³ G. Simi,⁴³ J. M. Tuggle,⁴³ C. Dallapiccola,⁴⁴ S. S. Hertzbach,⁴⁴ X. Li,⁴⁴ T. B. Moore,⁴⁴ E. Salvati,⁴⁴ S. Saremi,⁴⁴ R. Cowan,⁴⁵ D. Dujmic,⁴⁵ P. H. Fisher,⁴⁵ K. Koeneke,⁴⁵ G. Sciolla,⁴⁵ M. Spitznagel,⁴⁵ F. Taylor,⁴⁵ R. K. Yamamoto,⁴⁵ M. Zhao,⁴⁵ Y. Zheng,⁴⁵ S. E. Mclachlin,^{46,*} P. M. Patel,⁴⁶ S. H. Robertson,⁴⁶ A. Lazzaro,⁴⁷ F. Palombo,⁴⁷ J. M. Bauer,⁴⁸ L. Cremaldi,⁴⁸ V. Eschenburg,⁴⁸ R. Godang,⁴⁸ R. Kroeger,⁴⁸ D. A. Sanders,⁴⁸ D. J. Summers,⁴⁸ H. W. Zhao,⁴⁸ S. Brunet,⁴⁹ D. Côté,⁴⁹ M. Simard,⁴⁹ P. Taras,⁴⁹ F. B. Viaud,⁴⁹ H. Nicholson,⁵⁰ G. De Nardo,⁵¹ F. Fabozzi,^{51,§} L. Lista,⁵¹ D. Monorchio,⁵¹ C. Sciacca,⁵¹ M. A. Baak,⁵² G. Raven,⁵² H. L. Snoek,⁵² C. P. Jessop,⁵³ K. J. Knoepfel,⁵³ J. M. LoSecco,⁵³ G. Benelli,⁵⁴ L. A. Corwin,⁵⁴ K. Honscheid,⁵⁴ H. Kagan,⁵⁴ R. Kass,⁵⁴ J. P. Morris,⁵⁴ A. M. Rahimi,⁵⁴ J. J. Regensburger,⁵⁴ S. J. Sekula,⁵⁴ Q. K. Wong,⁵⁴ N. L. Blount,⁵⁵ J. Brau,⁵⁵ R. Frey,⁵⁵ O. Igonkina,⁵⁵ J. A. Kolb,⁵⁵ M. Lu,⁵⁵ R. Rahmat,⁵⁵ N. B. Sinev,⁵⁵ D. Strom,⁵⁵ J. Strube,⁵⁵ E. Torrence,⁵⁵ N. Gagliardi,⁵⁶ A. Gaz,⁵⁶ M. Margoni,⁵⁶ M. Morandin,⁵⁶ A. Pompili,⁵⁶ M. Posocco,⁵⁶ M. Rotondo,⁵⁶ F. Simonetto,⁵⁶ R. Stroili,⁵⁶ C. Voci,⁵⁶ E. Ben-Haim,⁵⁷ H. Briand,⁵⁷ G. Calderini,⁵⁷ J. Chauveau,⁵⁷ P. David,⁵⁷ L. Del Buono,⁵⁷ Ch. de la Vaissière,⁵⁷ O. Hamon,⁵⁷ Ph. Leruste,⁵⁷ J. Malcès,⁵⁷ J. Ocariz,⁵⁷ A. Perez,⁵⁷ J. Prendki,⁵⁷ L. Gladney,⁵⁸ M. Biasini,⁵⁹ R. Covarelli,⁵⁹ E. Manoni,⁵⁹ C. Angelini,⁶⁰ G. Batignani,⁶⁰

S. Bettarini,⁶⁰ M. Carpinelli,^{60,||} R. Cenci,⁶⁰ A. Cervelli,⁶⁰ F. Forti,⁶⁰ M. A. Giorgi,⁶⁰ A. Lusiani,⁶⁰ G. Marchiori,⁶⁰ M. A. Mazur,⁶⁰ M. Morganti,⁶⁰ N. Neri,⁶⁰ E. Paoloni,⁶⁰ G. Rizzo,⁶⁰ J. J. Walsh,⁶⁰ J. Biesiada,⁶¹ P. Elmer,⁶¹ Y. P. Lau,⁶¹ C. Lu,⁶¹ J. Olsen,⁶¹ A. J. S. Smith,⁶¹ A. V. Telnov,⁶¹ E. Baracchini,⁶² F. Bellini,⁶² G. Cavoto,⁶² D. del Re,⁶² E. Di Marco,⁶² R. Faccini,⁶² F. Ferrarotto,⁶² F. Ferroni,⁶² M. Gaspero,⁶² P. D. Jackson,⁶² M. A. Mazzoni,⁶² S. Morganti,⁶² G. Piredda,⁶² F. Polci,⁶² F. Renga,⁶² C. Voena,⁶² M. Ebert,⁶³ T. Hartmann,⁶³ H. Schröder,⁶³ R. Waldi,⁶³ T. Adye,⁶⁴ G. Castelli,⁶⁴ B. Franek,⁶⁴ E. O. Olaiya,⁶⁴ W. Roethel,⁶⁴ F. F. Wilson,⁶⁴ S. Emery,⁶⁵ M. Escalier,⁶⁵ A. Gaidot,⁶⁵ S. F. Ganzhur,⁶⁵ G. Hamel de Monchenault,⁶⁵ W. Kozanecki,⁶⁵ G. Vasseur,⁶⁵ Ch. Yèche,⁶⁵ M. Zito,⁶⁵ X. R. Chen,⁶⁶ H. Liu,⁶⁶ W. Park,⁶⁶ M. V. Purohit,⁶⁶ R. M. White,⁶⁶ J. R. Wilson,⁶⁶ M. T. Allen,⁶⁷ D. Aston,⁶⁷ R. Bartoldus,⁶⁷ P. Bechtle,⁶⁷ R. Claus,⁶⁷ J. P. Coleman,⁶⁷ M. R. Convery,⁶⁷ J. C. Dingfelder,⁶⁷ J. Dorfan,⁶⁷ G. P. Dubois-Felsmann,⁶⁷ W. Dunwoodie,⁶⁷ R. C. Field,⁶⁷ T. Glanzman,⁶⁷ S. J. Gowdy,⁶⁷ M. T. Graham,⁶⁷ P. Grenier,⁶⁷ C. Hast,⁶⁷ W. R. Innes,⁶⁷ J. Kaminski,⁶⁷ M. H. Kelsey,⁶⁷ H. Kim,⁶⁷ P. Kim,⁶⁷ M. L. Kocian,⁶⁷ D. W. G. S. Leith,⁶⁷ S. Li,⁶⁷ S. Luitz,⁶⁷ V. Luth,⁶⁷ H. L. Lynch,⁶⁷ D. B. MacFarlane,⁶⁷ H. Marsiske,⁶⁷ R. Messner,⁶⁷ D. R. Muller,⁶⁷ S. Nelson,⁶⁷ C. P. O'Grady,⁶⁷ I. Ofte,⁶⁷ A. Perazzo,⁶⁷ M. Perl,⁶⁷ T. Pulliam,⁶⁷ B. N. Ratcliff,⁶⁷ A. Roodman,⁶⁷ A. A. Salnikov,⁶⁷ R. H. Schindler,⁶⁷ J. Schwiening,⁶⁷ A. Snyder,⁶⁷ D. Su,⁶⁷ M. K. Sullivan,⁶⁷ K. Suzuki,⁶⁷ S. K. Swain,⁶⁷ J. M. Thompson,⁶⁷ J. Va'vra,⁶⁷ A. P. Wagner,⁶⁷ M. Weaver,⁶⁷ W. J. Wisniewski,⁶⁷ M. Wittgen,⁶⁷ D. H. Wright,⁶⁷ A. K. Yarritu,⁶⁷ K. Yi,⁶⁷ C. C. Young,⁶⁷ V. Ziegler,⁶⁷ P. R. Burchat,⁶⁸ A. J. Edwards,⁶⁸ S. A. Majewski,⁶⁸ T. S. Miyashita,⁶⁸ B. A. Petersen,⁶⁸ L. Wilden,⁶⁸ S. Ahmed,⁶⁹ M. S. Alam,⁶⁹ R. Bula,⁶⁹ J. A. Ernst,⁶⁹ B. Pan,⁶⁹ M. A. Saeed,⁶⁹ F. R. Wappler,⁶⁹ S. B. Zain,⁶⁹ S. M. Spanier,⁷⁰ B. J. Wogland,⁷⁰ R. Eckmann,⁷¹ J. L. Ritchie,⁷¹ A. M. Ruland,⁷¹ C. J. Schilling,⁷¹ R. F. Schwitters,⁷¹ J. M. Izen,⁷² X. C. Lou,⁷² S. Ye,⁷² F. Bianchi,⁷³ F. Gallo,⁷³ D. Gamba,⁷³ M. Pelliccioni,⁷³ M. Bomben,⁷⁴ L. Bosisio,⁷⁴ C. Cartaro,⁷⁴ F. Cossutti,⁷⁴ G. Della Ricca,⁷⁴ L. Lanceri,⁷⁴ L. Vitale,⁷⁴ V. Azzolini,⁷⁵ N. Lopez-March,⁷⁵ F. Martinez-Vidal,^{75,||} D. A. Milanes,⁷⁵ A. Oyanguren,⁷⁵ J. Albert,⁷⁶ Sw. Banerjee,⁷⁶ B. Bhuyan,⁷⁶ K. Hamano,⁷⁶ R. Kowalewski,⁷⁶ I. M. Nugent,⁷⁶ J. M. Roney,⁷⁶ R. J. Sobie,⁷⁶ P. F. Harrison,⁷⁷ J. Ilic,⁷⁷ T. E. Latham,⁷⁷ G. B. Mohanty,⁷⁷ H. R. Band,⁷⁸ X. Chen,⁷⁸ S. Dasu,⁷⁸ K. T. Flood,⁷⁸ J. J. Hollar,⁷⁸ P. E. Kutter,⁷⁸ Y. Pan,⁷⁸ M. Pierini,⁷⁸ R. Prepost,⁷⁸ S. L. Wu,⁷⁸ and H. Neal⁷⁹

(BABAR Collaboration)

¹Laboratoire de Physique des Particules, IN2P3/CNRS et Université de Savoie, F-74941 Annecy-Le-Vieux, France

²Universitat de Barcelona, Facultat de Física, Departament ECM, E-08028 Barcelona, Spain

³Università di Bari, Dipartimento di Fisica and INFN, I-70126 Bari, Italy

⁴University of Bergen, Institute of Physics, N-5007 Bergen, Norway

⁵Lawrence Berkeley National Laboratory and University of California, Berkeley, California 94720, USA

⁶University of Birmingham, Birmingham, B15 2TT, United Kingdom

⁷Ruhr Universität Bochum, Institut für Experimentalphysik 1, D-44780 Bochum, Germany

⁸University of Bristol, Bristol BS8 1TL, United Kingdom

⁹University of British Columbia, Vancouver, British Columbia, Canada V6T 1Z1

¹⁰Brunel University, Uxbridge, Middlesex UB8 3PH, United Kingdom

¹¹Budker Institute of Nuclear Physics, Novosibirsk 630090, Russia

¹²University of California at Irvine, Irvine, California 92697, USA

¹³University of California at Los Angeles, Los Angeles, California 90024, USA

¹⁴University of California at Riverside, Riverside, California 92521, USA

¹⁵University of California at San Diego, La Jolla, California 92093, USA

¹⁶University of California at Santa Barbara, Santa Barbara, California 93106, USA

¹⁷University of California at Santa Cruz, Institute for Particle Physics, Santa Cruz, California 95064, USA

¹⁸California Institute of Technology, Pasadena, California 91125, USA

¹⁹University of Cincinnati, Cincinnati, Ohio 45221, USA

²⁰University of Colorado, Boulder, Colorado 80309, USA

²¹Colorado State University, Fort Collins, Colorado 80523, USA

²²Universität Dortmund, Institut für Physik, D-44221 Dortmund, Germany

²³Technische Universität Dresden, Institut für Kern- und Teilchenphysik, D-01062 Dresden, Germany

²⁴Laboratoire Leprince-Ringuet, CNRS/IN2P3, Ecole Polytechnique, F-91128 Palaiseau, France

²⁵University of Edinburgh, Edinburgh EH9 3JZ, United Kingdom

²⁶Università di Ferrara, Dipartimento di Fisica and INFN, I-44100 Ferrara, Italy

²⁷Laboratori Nazionali di Frascati dell'INFN, I-00044 Frascati, Italy

²⁸Università di Genova, Dipartimento di Fisica and INFN, I-16146 Genova, Italy

²⁹Harvard University, Cambridge, Massachusetts 02138, USA

³⁰Universität Heidelberg, Physikalisches Institut, Philosophenweg 12, D-69120 Heidelberg, Germany

- ³¹Imperial College London, London, SW7 2AZ, United Kingdom
³²University of Iowa, Iowa City, Iowa 52242, USA
³³Iowa State University, Ames, Iowa 50011-3160, USA
³⁴Johns Hopkins University, Baltimore, Maryland 21218, USA
³⁵Universität Karlsruhe, Institut für Experimentelle Kernphysik, D-76021 Karlsruhe, Germany
³⁶Laboratoire de l'Accélérateur Linéaire, IN2P3/CNRS et Université Paris-Sud 11, Centre Scientifique d'Orsay, B. P. 34, F-91898 ORSAY Cedex, France
³⁷Lawrence Livermore National Laboratory, Livermore, California 94550, USA
³⁸University of Liverpool, Liverpool L69 7ZE, United Kingdom
³⁹Queen Mary, University of London, E1 4NS, United Kingdom
⁴⁰University of London, Royal Holloway and Bedford New College, Egham, Surrey TW20 0EX, United Kingdom
⁴¹University of Louisville, Louisville, Kentucky 40292, USA
⁴²University of Manchester, Manchester M13 9PL, United Kingdom
⁴³University of Maryland, College Park, Maryland 20742, USA
⁴⁴University of Massachusetts, Amherst, Massachusetts 01003, USA
⁴⁵Massachusetts Institute of Technology, Laboratory for Nuclear Science, Cambridge, Massachusetts 02139, USA
⁴⁶McGill University, Montréal, Québec, Canada H3A 2T8
⁴⁷Università di Milano, Dipartimento di Fisica and INFN, I-20133 Milano, Italy
⁴⁸University of Mississippi, University, Mississippi 38677, USA
⁴⁹Université de Montréal, Physique des Particules, Montréal, Québec, Canada H3C 3J7
⁵⁰Mount Holyoke College, South Hadley, Massachusetts 01075, USA
⁵¹Università di Napoli Federico II, Dipartimento di Scienze Fisiche and INFN, I-80126, Napoli, Italy
⁵²NIKHEF, National Institute for Nuclear Physics and High Energy Physics, NL-1009 DB Amsterdam, The Netherlands
⁵³University of Notre Dame, Notre Dame, Indiana 46556, USA
⁵⁴Ohio State University, Columbus, Ohio 43210, USA
⁵⁵University of Oregon, Eugene, Oregon 97403, USA
⁵⁶Università di Padova, Dipartimento di Fisica and INFN, I-35131 Padova, Italy
⁵⁷Laboratoire de Physique Nucléaire et de Hautes Energies, IN2P3/CNRS, Université Pierre et Marie Curie-Paris6, Université Denis Diderot-Paris7, F-75252 Paris, France
⁵⁸University of Pennsylvania, Philadelphia, Pennsylvania 19104, USA
⁵⁹Università di Perugia, Dipartimento di Fisica and INFN, I-06100 Perugia, Italy
⁶⁰Università di Pisa, Dipartimento di Fisica, Scuola Normale Superiore and INFN, I-56127 Pisa, Italy
⁶¹Princeton University, Princeton, New Jersey 08544, USA
⁶²Università di Roma La Sapienza, Dipartimento di Fisica and INFN, I-00185 Roma, Italy
⁶³Universität Rostock, D-18051 Rostock, Germany
⁶⁴Rutherford Appleton Laboratory, Chilton, Didcot, Oxon, OX11 0QX, United Kingdom
⁶⁵DSM/Dapnia, CEA/Saclay, F-91191 Gif-sur-Yvette, France
⁶⁶University of South Carolina, Columbia, South Carolina 29208, USA
⁶⁷Stanford Linear Accelerator Center, Stanford, California 94309, USA
⁶⁸Stanford University, Stanford, California 94305-4060, USA
⁶⁹State University of New York, Albany, New York 12222, USA
⁷⁰University of Tennessee, Knoxville, Tennessee 37996, USA
⁷¹University of Texas at Austin, Austin, Texas 78712, USA
⁷²University of Texas at Dallas, Richardson, Texas 75083, USA
⁷³Università di Torino, Dipartimento di Fisica Sperimentale and INFN, I-10125 Torino, Italy
⁷⁴Università di Trieste, Dipartimento di Fisica and INFN, I-34127 Trieste, Italy
⁷⁵IFIC, Universitat de Valencia-CSIC, E-46071 Valencia, Spain
⁷⁶University of Victoria, Victoria, British Columbia, Canada V8W 3P6
⁷⁷Department of Physics, University of Warwick, Coventry CV4 7AL, United Kingdom
⁷⁸University of Wisconsin, Madison, Wisconsin 53706, USA
⁷⁹Yale University, New Haven, Connecticut 06511, USA

(Received 11 September 2007; published 15 January 2008)

We present measurements of the semileptonic decays $B^- \rightarrow D^0 \tau^- \bar{\nu}_\tau$, $B^- \rightarrow D^{*0} \tau^- \bar{\nu}_\tau$, $\bar{B}^0 \rightarrow D^+ \tau^- \bar{\nu}_\tau$, and $\bar{B}^0 \rightarrow D^{*+} \tau^- \bar{\nu}_\tau$, which are potentially sensitive to non-standard model amplitudes. The data sample comprises $232 \times 10^6 Y(4S) \rightarrow B\bar{B}$ decays collected with the BABAR detector. From a combined fit to B^- and \bar{B}^0 channels, we obtain the branching fractions $\mathcal{B}(B^- \rightarrow D\tau^- \bar{\nu}_\tau) = (0.86 \pm 0.24 \pm 0.11 \pm 0.06)\%$ and $\mathcal{B}(B^- \rightarrow D^* \tau^- \bar{\nu}_\tau) = (1.62 \pm 0.31 \pm 0.10 \pm 0.05)\%$ (normalized for the \bar{B}^0), where the uncertainties are statistical, systematic, and normalization-mode-related.

Semileptonic decays of B mesons to the τ lepton—the heaviest of the three charged leptons—provide a new source of information on standard model (SM) processes [1–3], as well as a new window on physics beyond the SM [4–8]. In the SM, semileptonic decays occur at tree level and are mediated by the W boson, but the large mass of the τ lepton provides sensitivity to additional amplitudes, such as those mediated by a charged Higgs boson. Experimentally, $b \rightarrow c\tau^-\bar{\nu}_\tau$ decays [9] are challenging because the final state contains not just one, but two or three neutrinos as a result of the τ decay.

Branching fractions for semileptonic B decays to τ leptons are predicted to be smaller than those for $\ell = e, \mu$ [10]. Calculations based on the SM predict $\mathcal{B}(\bar{B}^0 \rightarrow D^+\tau^-\bar{\nu}_\tau) = (0.69 \pm 0.04)\%$ and $\mathcal{B}(\bar{B}^0 \rightarrow D^{*+}\tau^-\bar{\nu}_\tau) = (1.41 \pm 0.07)\%$ [8], which account for most of the predicted inclusive rate $\mathcal{B}(B \rightarrow X_c\tau^-\bar{\nu}_\tau) = (2.30 \pm 0.25)\%$ [2] (here, X_c represents all hadronic final states from the $b \rightarrow c$ transition). Calculations [4–8] in multi-Higgs doublet models show that substantial departures, either positive or negative, from the SM decay rate could occur for $\mathcal{B}(B \rightarrow D\tau^-\bar{\nu}_\tau)$. Those for $\mathcal{B}(B \rightarrow D^*\tau^-\bar{\nu}_\tau)$, however, are expected to be smaller.

Theoretical predictions for semileptonic decays to exclusive final states require knowledge of the form factors, which parametrize the hadronic current as functions of $q^2 = (p_B - p_{D^{(*)}})^2$. For light leptons (e, μ), there is effectively one form factor for $B \rightarrow D\ell^-\bar{\nu}_\ell$, while there are three for $B \rightarrow D^*\ell^-\bar{\nu}_\ell$. If a τ lepton is produced instead, one additional form factor enters in each mode. The form factors for $B \rightarrow D^{(*)}\ell^-\bar{\nu}_\ell$ decays involving the light leptons have been measured [11]. Heavy quark symmetry (HQS) relations [12] allow one to express the two additional form factors for $B \rightarrow D^{(*)}\tau^-\bar{\nu}_\tau$ in terms of the form factors measurable from decays with the light leptons. With sufficient data, one could probe the additional form factors and test the HQS relations.

The first measurements of semileptonic b -hadron decays to τ leptons were performed by the LEP experiments [13] operating at the Z^0 resonance, yielding an average [14] inclusive branching fraction $\mathcal{B}(b_{\text{had}} \rightarrow X\tau^-\bar{\nu}_\tau) = (2.48 \pm 0.26)\%$, where b_{had} represents the mixture of b -hadrons produced in $Z^0 \rightarrow b\bar{b}$ decays. The Belle experiment has recently obtained $\mathcal{B}(\bar{B}^0 \rightarrow D^{*+}\tau^-\bar{\nu}_\tau) = (2.02^{+0.40}_{-0.37} \pm 0.37)\%$ [15].

We determine the branching fractions of four exclusive decay modes: $B^- \rightarrow D^0\tau^-\bar{\nu}_\tau$, $B^- \rightarrow D^{*0}\tau^-\bar{\nu}_\tau$, $\bar{B}^0 \rightarrow D^+\tau^-\bar{\nu}_\tau$, and $\bar{B}^0 \rightarrow D^{*+}\tau^-\bar{\nu}_\tau$, each of which is measured relative to the corresponding e and μ modes. To reconstruct the τ , we use the decays $\tau^- \rightarrow e^-\bar{\nu}_e\nu_\tau$ and $\tau^- \rightarrow \mu^-\bar{\nu}_\mu\nu_\tau$, which are experimentally most accessible. The main challenge of the measurement is to separate $B \rightarrow D^{(*)}\tau^-\bar{\nu}_\tau$ decays, which have three neutrinos, from $B \rightarrow D^{(*)}\ell^-\bar{\nu}_\ell$ decays, which have the same observable final-state particles but only one neutrino.

We analyze data collected with the $BABAR$ detector [16] at the PEP-II e^+e^- storage rings at the Stanford Linear Accelerator Center. The data sample used comprises 208.9 fb^{-1} of integrated luminosity recorded on the $Y(4S)$ resonance, yielding $232 \times 10^6 B\bar{B}$ decays.

The analysis strategy is to reconstruct the decays of both B mesons in the $Y(4S) \rightarrow B\bar{B}$ event, providing powerful constraints on unobserved particles. One B meson, denoted B_{tag} , is fully reconstructed in a purely hadronic decay chain. The remaining charged particles and photons are required to be consistent with the products of a $b \rightarrow c$ semileptonic B decay: a hadronic system, a $D^{(*)}$ meson, and a lepton (e or μ). The lepton may be either primary or from $\tau^- \rightarrow \ell^-\bar{\nu}_\ell\nu_\tau$. We calculate the missing four-momentum $p_{\text{miss}} = [p_{e^+e^-} - p_{\text{tag}} - p_{D^{(*)}} - p_\ell]$ of any particles recoiling against the observed $B_{\text{tag}} + D^{(*)}\ell$ system. A large peak at zero in $m_{\text{miss}}^2 = p_{\text{miss}}^2$ corresponds to semileptonic decays with one neutrino, whereas signal events form a broad tail out to $m_{\text{miss}}^2 \sim 8 (\text{GeV}/c^2)^2$. To separate signal and background events, we perform a fit to the joint distribution of m_{miss}^2 and the lepton momentum ($|\mathbf{p}_\ell^*|$) in the rest frame of the B meson. In signal events, the observed lepton is the daughter of the τ and typically has a soft spectrum; for most background events, this lepton typically has higher momentum.

We reconstruct B_{tag} candidates [17] in 1114 final states $B_{\text{tag}} \rightarrow D^{(*)}Y^\pm$. Tag-side $D^{(*)}$ candidates are reconstructed in 21 decay chains, and the Y^\pm system may consist of up to six light hadrons (π^\pm, π^0, K^\pm , or K_S^0). B_{tag} candidates are identified using two kinematic variables, $m_{\text{ES}} = \sqrt{s/4 - |\mathbf{p}_{\text{tag}}|^2}$ and $\Delta E = E_{\text{tag}} - \sqrt{s}/2$, where \sqrt{s} is the total e^+e^- energy, $|\mathbf{p}_{\text{tag}}|$ is the magnitude of the B_{tag} momentum, and E_{tag} is the B_{tag} energy, all defined in the e^+e^- center-of-mass frame. We require $m_{\text{ES}} > 5.27 \text{ GeV}/c^2$ and $|\Delta E| < 72 \text{ MeV}$, each corresponding to $\pm 4\sigma$ (standard deviations). We reconstruct B_{tag} candidates in about 0.3% to 0.5% of $B\bar{B}$ events.

For the B meson decaying semileptonically, we reconstruct $D^{(*)}$ candidates in the modes $D^0 \rightarrow K^-\pi^+$, $K^-\pi^+\pi^0$, $K^-\pi^+\pi^+\pi^-$, $K_S^0\pi^+\pi^-$; $D^+ \rightarrow K^-\pi^+\pi^+$, $K^-\pi^+\pi^+\pi^0$, $K_S^0\pi^+$, $K^-K^+\pi^+$; $D^{*0} \rightarrow D^0\pi^0$, $D^0\gamma$; and $D^{*+} \rightarrow D^0\pi^+$, $D^+\pi^0$. D (D^*) candidates are selected within 4σ of the D mass ($D^* - D$ mass difference), with σ typically 5–10 MeV/c^2 (1–2 MeV/c^2). Electron candidates must have lab-frame momentum $|\mathbf{p}_e| > 300 \text{ MeV}/c$; muon candidates must have an appropriate signature in the muon detector system, effectively requiring $|\mathbf{p}_\mu| \geq 600 \text{ MeV}/c$. The energy of electron candidates is corrected for bremsstrahlung energy loss if photons are found close to the electron direction.

We require that all charged tracks be associated with either the B_{tag} , $D^{(*)}$, or ℓ candidate. We compute E_{extra} , the sum of the energies of all photon candidates not associated with the $B_{\text{tag}} + D^{(*)}\ell$ candidate system, and we require

$E_{\text{extra}} < 150\text{--}300$ MeV, depending on the $D^{(*)}$ channel. We suppress hadronic events and combinatorial backgrounds by requiring $|\mathbf{p}_{\text{miss}}| > 200$ MeV/ c and $q^2 > 4$ (GeV/ c^2) 2 . If multiple candidate systems pass this selection, we select the one with the lowest value of E_{extra} . To improve the m_{miss}^2 resolution, we perform a kinematic fit to the event, constraining particle masses to known values and requiring tracks from B , D , and K_S^0 mesons to originate from appropriate common vertices. All event selection requirements and fit procedures have been defined using simulated events or using control samples in data that exclude the signal region.

Figure 1 shows the distributions of m_{miss}^2 for the four $D^{(*)}\ell$ channels, along with the projections of the maximum likelihood fit discussed below. We observe large peaks at $m_{\text{miss}}^2 \approx 0$ as well as events in the signal region at large m_{miss}^2 . The peaks are mainly due to $B \rightarrow D^{(*)}\ell^- \bar{\nu}_\ell$, which serve as normalization modes. The structure of this background is shown in the inset figures, which expand the region $-0.4 < m_{\text{miss}}^2 < 1.4$ (GeV/ c^2) 2 . $B \rightarrow D^{(*)}\ell^- \bar{\nu}_\ell$ background is the dominant feature in the two $D^{*}\ell$ channels [Figs. 1(a) and 1(c)]; the two $D\ell$ channels [Figs. 1(b) and 1(d)] are dominated by $B \rightarrow D\ell^- \bar{\nu}_\ell$ decays but also include substantial contributions from true D^* mesons where the low-momentum π^0 or photon from $D^* \rightarrow D\pi^0$ or $D\gamma$ is not reconstructed. Similarly, $B \rightarrow D^*\tau^- \bar{\nu}_\tau$ events can feed down to the $D\ell$ channels. The fit therefore includes feed-down components for both the signal and normalization modes, as well as smaller feed-up contributions from $B \rightarrow D(\ell^-/\tau^-)\bar{\nu}$ into the $D^{*}\ell$ channels. Other sources of background include $B \rightarrow D^{**}(\ell^-/\tau^-)\bar{\nu}$ events [here D^{**} represents charm resonances heavier than the $D^*(2010)$, as well as nonresonant $D^{(*)}n\pi$ systems with $n \geq 1$]; charge-crossfeed ($B \rightarrow D^{(*)}\ell^- \bar{\nu}_\ell$ events reconstructed with the wrong charge for the B_{tag} and $D^{(*)}$ meson, typically because a low-momentum π^\pm is swapped between them); and combinatorial background. This last background is dominated by hadronic B decays, such as $B \rightarrow D^{(*)}D_s^{(*)}$, that produce a secondary lepton, including τ leptons from D_s decay.

To constrain $B \rightarrow D^{**}(\ell^-/\tau^-)\bar{\nu}$ background, we select four control samples, identical to the signal channels but in which an extra π^0 meson is observed. Most of the D^{**} background in the signal channels occurs when the π^0 from $D^{**} \rightarrow D^{(*)}\pi^0$ is not reconstructed, so these control samples provide a normalization of the background source. D^{**} decays in which a π^\pm is lost do not have the correct charge correlation between the B_{tag} and $D^{(*)}$, and decays with two missing charged pions are rare. The feed-down probabilities for the $D^{**}(\ell^-/\tau^-)\bar{\nu}$ background are determined from simulation, with uncertainties in the D^{**} content treated as a systematic error.

We perform a relative measurement, extracting both signal $B \rightarrow D^{(*)}\tau^- \bar{\nu}_\tau$ and normalization $B \rightarrow D^{(*)}\ell^- \bar{\nu}_\ell$

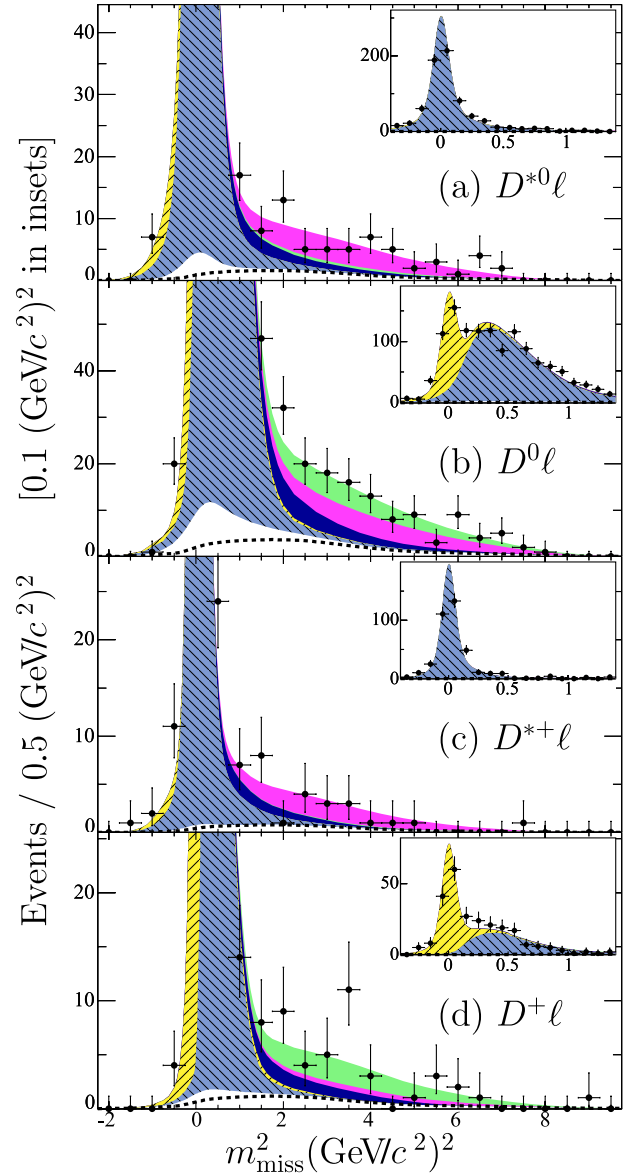


FIG. 1 (color online). Distributions of events and fit projections in m_{miss}^2 for the four final states: $D^{*0}\ell^-$, $D^0\ell^-$, $D^{*+}\ell^-$, and $D^+\ell^-$. The normalization region $m_{\text{miss}}^2 \approx 0$ is shown with finer binning in the insets. The fit components are combinatorial background (white, below dashed line), charge crossfeed background (white, above dashed line), the $B \rightarrow D\ell^- \bar{\nu}_\ell$ normalization mode ($//$ hatching, yellow), the $B \rightarrow D^{*}\ell^- \bar{\nu}_\ell$ normalization mode ($\backslash\backslash$ hatching, light blue), $B \rightarrow D^{*}\ell^- \bar{\nu}_\ell$ background (dark, or blue), the $B \rightarrow D\tau^- \bar{\nu}_\tau$ signal (light gray, green), and the $B \rightarrow D^{*}\tau^- \bar{\nu}_\tau$ signal (medium gray, magenta). The fit shown incorporates the $B^- - \bar{B}^0$ constraints.

yields from the fit to obtain the four branching ratios $R(D^0)$, $R(D^+)$, $R(D^{*0})$, and $R(D^{*+})$, where, for example, $R(D^{*0}) \equiv \mathcal{B}(B^- \rightarrow D^{*0}\tau^- \bar{\nu}_\tau)/\mathcal{B}(B^- \rightarrow D^{*0}\ell^- \bar{\nu}_\ell)$. These ratios are normalized such that ℓ represents only one of e or μ ; however, both light lepton species are included in the measurement. Signal and background yields are extracted

using an extended, unbinned maximum likelihood fit to the joint $(m_{\text{miss}}^2, |\mathbf{p}_\ell^*|)$ distribution. The 18-parameter fit is performed simultaneously in the four signal channels and the four D^{**} control samples. In each of the four signal channels, we describe the data as the sum of seven components (shown in Fig. 1): $D\tau^-\bar{\nu}_\tau$, $D^*\tau^-\bar{\nu}_\tau$, $D\ell^-\bar{\nu}_\ell$, $D^*\ell^-\bar{\nu}_\ell$, $D^{**}(\ell^-/\tau^-)\bar{\nu}$, charge crossfeed, and combinatorial background; these last two are fixed in the fit and varied as systematic errors. The four D^{**} control samples are described as the sum of five components: $D^{**}(\ell^-/\tau^-)\bar{\nu}$, $D\ell^-\bar{\nu}_\ell$, $D^*\ell^-\bar{\nu}_\ell$, charge crossfeed, and combinatorial background, with the charge crossfeed fixed in the fit. Probability distribution functions (PDFs) are determined from simulated event samples except for the parameters describing the amount of D^* feed-down into the D channels, which are determined directly by the fit. Both the signal and normalization modes are described using HQET-based form factors [18] for which the parameters and their uncertainties are determined by experimental measurements [11].

Table I summarizes the results from two fits, one in which all four signal yields can vary independently, and a second fit in which we constrain [20] $R(D^+) = R(D^0)$ and $R(D^{*+}) = R(D^{*0})$. The m_{miss}^2 projections shown in Fig. 1 are those from this $B^- - \bar{B}^0$ -constrained fit.

The features of the event sample have been extensively checked. The observed lepton spectra are well described by the fit both in signal- and in background-dominated regions. The properties of reconstructed B_{tag} mesons, such as charged and neutral daughter multiplicities, are consistent with expectations. Control samples of $B \rightarrow D^{(*)}\ell^-\bar{\nu}_\ell$ events, kinematically selected without a cut on m_{miss}^2 , provide checks of numerous distributions, including the m_{miss}^2 tails and E_{extra} .

Systematic uncertainties on R associated with the fit, $(\Delta R/R)_{\text{fit}}$ in Table I, are determined by running ensembles of fits in which input parameters are distributed according to our knowledge of the underlying source, and include the

PDF parametrization (2% to 12%); the composition of combinatorial backgrounds (2% to 11%); the mixture of D^{**} states in $B \rightarrow D^{**}\ell^-\bar{\nu}_\ell$ decays (0.3% to 6%); the $B \rightarrow D^*$ form factors (0.2% to 1.9%); the π^0 reconstruction efficiency, which affects the D^* and D^{**} feed-down rates (0.5% to 1.1%); and the m_{miss}^2 resolution for $B \rightarrow D^*\ell^-\bar{\nu}_\ell$ events (0.1% to 1.6%). Uncertainties on the $B \rightarrow D$ form factors contribute less than 1%. Uncertainties on R propagated from the ratio of efficiencies, $(\Delta R/R)_\varepsilon$ in Table I, are typically small due to cancellations, and include the limited statistics in the simulation (0.8% to 1.5%) and systematic errors related to detector performance (0.2% to 0.7%). Uncertainties from modeling final-state radiation are 0.3% to 0.5%; uncertainties on the branching fractions of the reconstructed modes contribute 0.3% or less. Finally, the uncertainty on $\mathcal{B}(\tau^- \rightarrow \ell^-\bar{\nu}_\ell\nu_\tau)$ [14] contributes 0.2% to all modes.

Table I gives the significances of the signal yields. The statistical significance is determined from $\sqrt{2\Delta(\ln\mathcal{L})}$, where $\Delta(\ln\mathcal{L})$ is the change in log-likelihood between the nominal fit and the no-signal hypothesis. The total significance is determined by including $(\Delta R/R)_{\text{fit}}$ in quadrature with the statistical error.

We have presented measurements of the decays $B \rightarrow D\tau^-\bar{\nu}_\tau$ and $B \rightarrow D^*\tau^-\bar{\nu}_\tau$, relative to the corresponding decays to light leptons. We find $R(D) = (41.6 \pm 11.7 \pm 5.2)\%$ and $R(D^*) = (29.7 \pm 5.6 \pm 1.8)\%$, where the first error is statistical and the second is systematic. Normalizing to known \bar{B}^0 branching fractions [19], we obtain

$$\mathcal{B}(B \rightarrow D\tau^-\bar{\nu}_\tau) = (0.86 \pm 0.24 \pm 0.11 \pm 0.06)\%$$

$$\mathcal{B}(B \rightarrow D^*\tau^-\bar{\nu}_\tau) = (1.62 \pm 0.31 \pm 0.10 \pm 0.05)\%,$$

where the third error is from that on the normalization mode branching fraction. The significances of the signals are 3.6σ and 6.2σ , respectively. The modes $B^- \rightarrow D^0\tau^-\bar{\nu}_\tau$, $B^- \rightarrow D^{*0}\tau^-\bar{\nu}_\tau$, and $\bar{B}^0 \rightarrow D^+\tau^-\bar{\nu}_\tau$ have not been studied previously, while the measurement of

TABLE I. Results from fits to data: the signal yield (N_{sig}), the yield of normalization $B \rightarrow D^{(*)}\ell^-\bar{\nu}_\ell$ events (N_{norm}), the ratio of signal and normalization mode efficiencies ($\varepsilon_{\text{sig}}/\varepsilon_{\text{norm}}$), the relative systematic error due to the fit yields [$(\Delta R/R)_{\text{fit}}$], the relative systematic error due to the efficiency ratios [$(\Delta R/R)_\varepsilon$], the branching fraction relative to the normalization mode (R), the absolute branching fraction (\mathcal{B}), and the total and statistical signal significances (σ_{tot} and σ_{stat}). The first two errors on R and \mathcal{B} are statistical and systematic, respectively; the third error on \mathcal{B} represents the uncertainty on the normalization mode [19]. The last two rows show the results of the fit with the $B^- - \bar{B}^0$ constraint applied, where \mathcal{B} is expressed for the \bar{B}^0 . The statistical correlation between $R(D)$ and $R(D^*)$ in this fit is -0.51 .

Mode	N_{sig}	N_{norm}	$\varepsilon_{\text{sig}}/\varepsilon_{\text{norm}}$	$(\Delta R/R)_{\text{fit}}$ [%]	$(\Delta R/R)_\varepsilon$ [%]	R [%]	\mathcal{B} [%]	σ_{tot} σ_{stat}
$B^- \rightarrow D^0\tau^-\bar{\nu}_\tau$	35.6 ± 19.4	347.9 ± 23.1	1.85	15.5	1.6	$31.4 \pm 17.0 \pm 4.9$	$0.67 \pm 0.37 \pm 0.11 \pm 0.07$	1.8 (1.8)
$B^- \rightarrow D^{*0}\tau^-\bar{\nu}_\tau$	92.2 ± 19.6	1629.9 ± 63.6	0.99	9.7	1.5	$34.6 \pm 7.3 \pm 3.4$	$2.25 \pm 0.48 \pm 0.22 \pm 0.17$	5.3 (5.8)
$\bar{B}^0 \rightarrow D^+\tau^-\bar{\nu}_\tau$	23.3 ± 7.8	150.2 ± 13.3	1.83	13.9	1.8	$48.9 \pm 16.5 \pm 6.9$	$1.04 \pm 0.35 \pm 0.15 \pm 0.10$	3.3 (3.6)
$\bar{B}^0 \rightarrow D^{*+}\tau^-\bar{\nu}_\tau$	15.5 ± 7.2	482.3 ± 25.5	0.91	3.6	1.4	$20.7 \pm 9.5 \pm 0.8$	$1.11 \pm 0.51 \pm 0.04 \pm 0.04$	2.7 (2.7)
$B \rightarrow D\tau^-\bar{\nu}_\tau$	66.9 ± 18.9	497.8 ± 26.4	-	12.4	1.4	$41.6 \pm 11.7 \pm 5.2$	$0.86 \pm 0.24 \pm 0.11 \pm 0.06$	3.6 (4.0)
$B \rightarrow D^*\tau^-\bar{\nu}_\tau$	101.4 ± 19.1	2111.5 ± 68.1	-	5.8	1.3	$29.7 \pm 5.6 \pm 1.8$	$1.62 \pm 0.31 \pm 0.10 \pm 0.05$	6.2 (6.5)

$\bar{B}^0 \rightarrow D^{*+} \tau^- \bar{\nu}_\tau$ is consistent with the Belle result [15]. The averaged branching fractions are about 1σ higher than the SM predictions but, given the uncertainties, there is still room for a sizeable non-SM contribution.

We are grateful for the excellent luminosity and machine conditions provided by our PEP-II colleagues, and for the substantial dedicated effort from the computing organizations that support *BABAR*. The collaborating institutions wish to thank SLAC for its support and kind hospitality. This work is supported by DOE and NSF (USA), NSERC (Canada), CEA and CNRS-IN2P3 (France), BMBF and DFG (Germany), INFN (Italy), FOM (The Netherlands), NFR (Norway), MIST (Russia), MEC (Spain), and STFC (United Kingdom). Individuals have received support from the Marie Curie EIF (European Union) and the A. P. Sloan Foundation.

*Deceased.

†Present address: Tel Aviv University, Tel Aviv, 69978, Israel.

‡Also with Università di Perugia, Dipartimento di Fisica, Perugia, Italy.

§Also with Università della Basilicata, Potenza, Italy.

||Also with Università di Sassari, Sassari, Italy.

¶Also with Universitat de Barcelona, Facultat de Física, Departament ECM, E-08028 Barcelona, Spain.

- [1] J. G. Körner and G. A. Schuler, Phys. Lett. B **231**, 306 (1989); Z. Phys. C **46**, 93 (1990).
- [2] A. F. Falk *et al.*, Phys. Lett. B **326**, 145 (1994).
- [3] D. S. Hwang and D.-W. Kim, Eur. Phys. J. C **14**, 271 (2000).
- [4] B. Grzadkowski and W.-S. Hou, Phys. Lett. B **283**, 427 (1992).
- [5] M. Tanaka, Z. Phys. C **67**, 321 (1995).
- [6] K. Kiers and A. Soni, Phys. Rev. D **56**, 5786 (1997).
- [7] H. Itoh, S. Komine, and Y. Okada, Prog. Theor. Phys. **114**, 179 (2005).
- [8] C.-H. Chen and C.-Q. Geng, J. High Energy Phys. **10** (2006) 053.
- [9] Charge-conjugate modes are implied throughout.
- [10] Throughout this Letter, we use the symbol ℓ to refer only to the light charged leptons e and μ . The symbol $D^{(*)}$ refers either to a D or a D^* meson.
- [11] J. E. Duboscq *et al.* (CLEO Collab.), Phys. Rev. Lett. **76**, 3898 (1996); B. Aubert *et al.* (*BABAR* Collaboration), Phys. Rev. D **74**, 092004 (2006); E. Barberio *et al.* (HFAG), arXiv:0704.3575.
- [12] N. Isgur and M. B. Wise, Phys. Lett. B **232**, 113 (1989); **237**, 527 (1990).
- [13] M. Acciari *et al.* (L3 Collaboration), Phys. Lett. B **332**, 201 (1994); Z. Phys. C **71**, 379 (1996); R. Barate *et al.* (ALEPH Collaboration), Eur. Phys. J. C **19**, 213 (2001); G. Abbiendi *et al.* (OPAL Collaboration), Phys. Lett. B **520**, 1 (2001).
- [14] W.-M. Yao *et al.* (Particle Data Group), J. Phys. G **33**, 1 (2006).
- [15] A. Matyja *et al.* (Belle Collaboration), Phys. Rev. Lett. **99**, 191807 (2007).
- [16] B. Aubert *et al.* (*BABAR* Collaboration), Nucl. Instrum. Methods Phys. Res., Sect. A **479**, 1 (2002).
- [17] B. Aubert *et al.* (*BABAR* Collaboration), Phys. Rev. Lett. **92**, 071802 (2004).
- [18] I. Caprini, L. Lellouch, and M. Neubert, Nucl. Phys. B **530**, 153 (1998).
- [19] We use [14] to normalize the four individual branching fractions. For the $B^- - \bar{B}^0$ -constrained measurement, we use our own averages of the values in [14]: $\mathcal{B}(\bar{B}^0 \rightarrow D^+ \ell^- \bar{\nu}_\ell) = (2.07 \pm 0.14)\%$ and $\mathcal{B}(\bar{B}^0 \rightarrow D^{*+} \ell^- \bar{\nu}_\ell) = (5.46 \pm 0.18)\%$.
- [20] This constraint follows from isospin symmetry in both the signal and normalization modes but is more general.